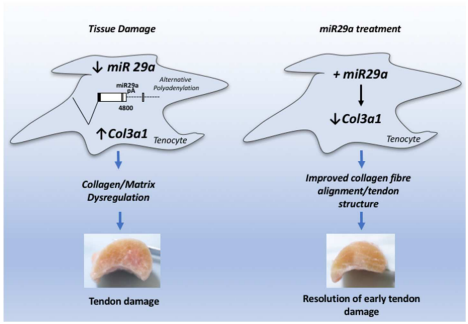
Tissue Damage
↓ miR 29a
miR29a
GA
4800
Alternative
Polyadenylation
↑Col3a1
Tenocyte
Collagen/Matrix
Dysregulation
Tendon damage
miR29a treatment
+ miR29a
↓Col3a1
Tenocyte
Improved collagen fibre
alignment/tendon
structure
Resolution of early tendon
damage

microRNA29a treatment improves early tendon injury

Ashlee E Watts[1†],Neal L Millar[2†], Josh Platt[1], Susan M Kitson[2], Moeed Akbar[2], Raquel Rech[1], Jay Griffin[1], Roy Pool[1], Tom Hughes[3], Iain B McInnes[2], D. S. Gilchrist[2].

[1] The Comparative Orthopedics and Regenerative Medicine Laboratory, Texas A&M University.

[2] Institute of Infection, Immunity and Inflammation, College of Medicine, Veterinary and Life Sciences University of Glasgow, Glasgow, Scotland UK

[3] Liphook Equine Hospital, Forest Mere, Liphook, Hampshire, United Kingdom

[†] Authors contributed equally to this work

Correspondence:

Dr Derek S Gilchrist PhD and Mr Neal L Millar PhD FRCSEd(Tr&Ortho)
Institute of Infection, Immunity and Inflammation,
College of Medicine, Veterinary and Life Sciences
University of Glasgow
120 University Avenue
Glasgow G12 8TA
Tel: +44 141 330 8134
Fax: +44 141 330 8420
Email: derek.gilchrist@glasgow.ac.uk and neal.millar@glasgow.ac.uk

Summary sentence

This work highlights a *microRNA* replacement therapy as a therapeutic option for tendon injury.

Abstract

Tendon injuries (tendinopathies) are common in human and equine athletes and characterised by dysregulated collagen matrix resulting in tendon damage. We have previously demonstrated a functional role for miR29a as a post-transcriptional regulator of collagen 3 expression in murine and human tendon injury. Given the translational potential, we designed a randomised, blinded trial to evaluate the potential of a miR29a replacement therapy as a therapeutic option to treat tendinopathy in an equine model which closely mimics human disease. Tendon injury was induced in the superficial digital flexor tendon (SDFT) of 17 horses. Tendon lesions were treated one week later with an intralesional injection of miR29a or placebo. miR29a treatment reduced collagen 3 transcript levels at week 2 with no significant changes in collagen 1. Relative lesion cross-sectional area was significantly lower in miR29a tendons compared to control tendons. Histology scores were significantly better for miR29a treated tendons compared to control tendons. This data supports the mechanism of miRNA-mediated modulation of the early pathophysiologic events that facilitate tissue remodelling in the tendon after injury and provides strong proof of principle that a locally delivered miR29a therapy improves early tendon healing.

Keywords

MicroRNA 29a, Tendon, Tendinopathy, Inflammation, Equine

Introduction

Dysregulated tissue repair and inflammation characterize many musculoskeletal pathologies, including tendon disorders in both human and equine practice[1-4]. Tendon injuries remain a significant problem in equine practice comprising the most common musculoskeletal injury in racehorses. Injury to the SDFT, most often involving the metacarpal segment of the forelimb tendon, is one of the most frequent causes of lameness of athletic horses internationally with a reported frequency of 10–30%[5,6].

The immune system plays a crucial role in the regulation of tissue remodelling by coordinating complex signalling networks that facilitate transcriptional regulation of extracellular matrix (ECM) components as an adaptive response to environmental cues. Inflammatory mediators are considered crucial to the onset and perpetuation of tendinopathy[7-9]. Expression of various cytokines has been demonstrated in inflammatory cell lineages and tenocytes, suggesting that both infiltrating and resident populations participate in pathology[10-12]. Additionally, evidence suggests a balance exists between pro inflammatory and pro resolving mediators that may ultimately define the extent to which equine tendinopathy develops and subsequently repairs[13,14].

Recent work has identified the importance of tissue microenvironments and the interaction immune mediators in inflammatory/ stromal cell crosstalk[15]. MicroRNAs (miRNAs) are small, non-coding RNAs that suppress gene expression at the post-transcriptional level by inhibiting translation and/or inducing mRNA degradation[16]. A single miRNA can regulate the expression of multiple target mRNAs through sequence binding. Emerging studies highlight miRNAs as key epigenetic regulators of integrated mammalian cell functions[17,18]. Specific miRNAs have emerged that particularly regulate cytokine networks while orchestrating proliferation and differentiation of stromal lineages that determine ECM composition[19]. miRNAs have provoked extensive interest as regulators of musculoskeletal diseases, although their precise contributions to complex disease pathways remains uncertain[20]. miR-210 has been reported as a crucial regulator of angiogenesis[21], a key factor in tendon disease, and it accelerated healing of

tendon in an Achilles tendon rodent injury model[22] while additionally causing upregulation of vascular endothelial factor, fibroblast growth factor and type I collagen in the same model system. miRNAs designed and engineered according to genetic sequences of transforming growth factor β1 (TGFβ1) and injected in the chicken tendon injury model achieved downregulation of TGFβ1 expression *in vitro* and *in vivo*[23]. Some compounds can regulate endogenous miRNA expression, which may confer therapeutic value. One such study demonstrated that miR29b mediated chitosan-induced prevention of tendon adhesion after rodent Achilles tendon injury surgery by regulating the TGFβ1–Smad3 pathway[24].

We have previously demonstrated a functional role for miR29a as a post-transcriptional regulator of collagen in murine and human tendon injury[25]. Given the translational potential we designed a randomized blinded trial to evaluate the potential for miR29a replacement therapy as a therapeutic option to treat tendinopathy utilising an equine collagenase model considered analogous to human tendon disease.

Results

miR29a expression in equine tendinopathy model

We found that miR29a was significantly ($p<0.01$) downregulated throughout the time course of the induced tendinopathy model (Figure 1a). Additionally, we noted a significant differential regulation of collagen 1 and 3 transcripts throughout the time course (Figure 1b &c). The most notable changes were in collagen 3 transcript early in the model, which was upregulated 80 fold at week 3 and 25 fold at week 5 post induction which was maintained >30 fold at weeks 9 and 17. This was in contrast to Collagen 1 transcripts which were upregulated significantly less ($p<0.05$) at early time points (13 fold at 3 weeks, 9 fold at 5 weeks, $p<0.05$ versus collagen 3 transcript) which was reversed at weeks 9 (26 fold) and 17 (24 fold).

Regulation of collagen expression by miR29a is conserved in equine tenocytes

Sequence analysis revealed that the miR29a binding sites in collagen 1 and 3 transcripts previously described in humans and mice are conserved in horses (Figures 1 d-e). To confirm the activities of these predicted miR29a binding sites a series of luciferase reporter constructs containing wild-type and mutated miR29a-bindings sites were made. Over-expression of miR29a decreased luciferase activity in HEK cells transfected with in wild-type but not mutated plasmids demonstrating that both col1a1 and col3a1 are bone fide miR29a targets (Figure 1 f-g). To test whether miR29a indeed regulates the levels of candidate target mRNAs in disease-relevant cells, we transfected primary equine tenocytes with miR29a mimic. miR29a manipulation selectively regulated collagen 3 ($p<0.01$) but not collagen 1 mRNA (Figure 2 a-b). This in is keeping with our previous observations in human tenocytes which showed that miR29a binding sites are excised from collagen 1 transcripts due to the use of an alternative proximal polyadenylation signal[25]. Comparison of the polyA sites in both col1a1 and col3a1 showed that the polyadenylation signals and the sequences that flank them are identical in

other mammalian species including horses and dogs, suggesting that this alternative polyadenylation is conserved in these species (Figure 2 c-f). To test this, the 3' ends of collagen1 and 3 transcripts were characterised using 3'RACE. Sequence analysis showed that both collagen1 and 3 utilised the same conserved polyadenylation signals found in the corresponding human transcripts (Figure 2 g-h). Together these results support the idea of common molecular pathogenic process driven by the loss of miR29a in the development of tendinopathy in human and horses. This finding raises the possibility that re-introduction of miR29a could have significant therapeutic benefit in the healing of tendon lesions.

miR29a treatment improves early tendon healing

The study consisted of two randomly assigned groups: group A (miRNA29a mimic; n =9 ; 5 male, 4 female; miRNA29a) and group B (placebo treated tendons; n = 8; 5 male, 3 female; CONT) with the study timeline detailed in Figure 3a.

Quantitative PCR : miR29a treatment specifically suppressed collagen 3 at week 2 ($p=0.01$) and showed a trend toward reduction at week 4 ($p=0.06$) (Figure 3 b-c). Importantly in keeping with our in vitro data miR29a treatment caused no significant changes in collagen 1 at any time points in this equine model.

Ultrasound: Normalized lesion CSA was significantly lower in miR29a treated tendons compared to control tendons at t = 6,12 &16 weeks ($p<0.05$) and showed a trend for smaller CSA at t = 8 weeks ($p = 0.1$) (Figure 4a). Normalized relative lesion CSA was significantly lower in miR29a tendons compared to control tendons at t = 6,8,12 &16 weeks ($p<0.05$) (Figure 4b). Subjective blinded US scoring showed significant less SC thickening and more normal tissue architecture at week 12 & 16 in the miR29a tendons compared to control tendons (Figure 4c and Table 1).

MRI: Tendon lesions were identified by increased T2-weighted signal intensity in all tendons (Figure 5a-b). Tendon CSA made on MR images were not significantly different between groups (Figure 5b). However, there was a trend ($p=0.07$) of reduced relative CSA and reduced lesion CSA of miR29a treated tendons compared to that of control tendons at weeks 4,6,12 &16. Additionally, the T_2 relaxation times was significantly ($p<0.05$) greater in control tendons at 12 weeks (mir29a; 57.9 ± 15, control; 218.9 ± 74.6) (Figure 5c).

Gross dissection & Histology: No peritendinous adhesions were noted during dissection in either group. Cumulative histology scores were significantly better for miR29a treated tendons compared to control tendons (Figure 6a and b) at weeks 2 & 16 utilizing the modified Bonar score (Cell density, vascularity, linear fibre and polarised collagen). Tendons from both groups were visibly enlarged, centered at 16 cm DACB, and had minimal peri-tendinous reaction. Although no scores were assigned, miR29a treated tendons appeared smaller at 16 cm DACB, had less peri-tendinous reaction and treatment injection sites were less obvious (Figure 6c).

Discussion

The molecular processes underpinning the development of collagen 3 over-production seen in tendinopathy have been evolutionarily conserved in mammalian species demonstrating their biological importance. Here we showed that the injury-induced loss of miR29a from tenocytes previously reported in humans also occurs in collagenase-induced tendinopathy in horses and that this inversely correlates with collagen 3 expression. We have demonstrated that as is the case in humans, miR29a has the potential to target both collagen 1 and 3. Despite this, only collagen 3 expression is decreased by the miR29a overexpression in equine tenocytes. A detailed characterisation of col1a1 and col3a1 transcripts reveals that col1a1 utilises an alternative polyA signal that truncates its 3'UTR with the loss of all three miR29 binding sites. This means that in equine tenocytes only collagen 3 is regulated by miR29a, a situation that mirrors that previously described in humans. These findings raised the possibility that re-introduction of miR29a into the tendinopathic environment could reduce collagen 3 production leading to improved tendon healing. To test this, we designed a blinded, placebo-controlled, experimental trial an equine model that revealed clinically relevant improvement in the healing of earlt tendon injury after intralesional injection of miR29a.

Recent studies highlight miRNAs as key regulators of leukocyte function and differentiation of stromal cells that determine extracellular matrix composition[20,26,27]. Our data demonstrate a functional role for miR29a as a post-transcriptional regulator of collagen in equine tendon injury. Despite its many similarities, the collagenase model of tendon injury does not totally mimic the insidious and degenerate etiopathogenesis of many forms of naturally occurring tendon injury in man. However, the clinical relevance of this model to the final acute disruption after months or years of chronic tendon injury, is supported by the evaluation of gross, biochemical and histopathological changes, clinical signs, mechanical characteristics, and MRI and ultrasonographic findings following the induction of injury[28,29]. Additionally, the collagenase model allows the generation of a homogenous tendon lesion in a controlled group of animals and, therefore, improved ability to detect

differences between treated and control arms of the study. The reduced expression of miR29a immediately after tendon injury up until 16 weeks post injury induction and concomitant increase in collagen 3:collagen 1 ratio in control animals that we report herein further demonstrates the model molecularly reflects disease in human and in rodent models of tendinopathy[25]. The regulation of collagens and other extracellular matrices by the miR29 family has been highlighted in several prior studies[17,25,30]. Our results now show that miR-29a acts as an important repressor to regulate collagen expression in equine tendon healing. The molecular understanding of increased collagen 3 deposition resulting in biomechanical inferiority and degeneration has been largely under investigated in equine tendon disease. While it is likely that miR29a targets other important genes[31,32] in the multifaceted tendon injury mileu, our data suggest that the miR29a is a critical driver of the collagen post transcriptional regulation resulting in a key collagen switch that remains a major pathological feature of equine tendinopathy. Novel quantitative biochemical MRI techniques, such as T2 mapping, have been increasingly evaluated for their demonstrated sensitivity in detection of earlier biochemical changes (i.e. collagen bril structure, orientation, and water content) in various tissues[33,34]. Thus the variability in T2 mapping of placebo treated tendons as compared to miR-29a treated tendons suggest improved tissue quality, collagen content and collagen orientation due to miR-29a replacement.

The standard of care for tendon and ligament injury in equine clinical medicine is conservative therapy, based on minimizing exercise and anti-inflammatory medication. Novel methods have focused on regenerative medicine approaches with either platelet rich plasma (PRP) or stem cells. None of these recent 'novel' tendinopathy treatments have provided mechanistic insight; thus, their wholehearted adoption in the clinical community is not yet apparent. Following PRP in the horse, there is experimental evidence of improved histology[35], increased neovascularization[36] and ultrasound appearance[37] of treated tendons but clinical evidence has failed to show a treatment effect[38], similar to the experience in human tendon disease[39]. Following stem cells in the horse, there is experimental evidence of improved histology[40,41] and clinical evidence for safety[42], improved cellularity[43] and a

reduced re-injury rate compared to historical controls[44] . The initial enthusiasm for stem cells in regenerative medicine was one of tissue specific differentiation in that stem cells implanted to a tendon lesion, for example, would engraft, become tenocytes and produce tendon matrix. As both basic science and clinical data accumulates, it appears that stem cell therapy with the mesenchymal stem cell is due to local production of bioactive molecules and immune modulation rather than tissue specific differentiation and long-term engraftment[45]. Herein, we show that local delivery of miR29a is capable of producing comparable and in some cases superior results to PRP or stem cell treatment (similar experimental trials) with regard to lesion size and histological improvement[46,47]. Our study appears to mirror the concept of earlier lesion resolution and lack of lesion progression at early time points. This in conjunction with a concurrent tissue molecular phenotype of reduced collagen 3 confirmed macroscopically on T2 mapping provides convincing evidence that a miR manipulation can target both inflammatory/matrix crosstalk in tendon disease with subsequent lesion resolution. miRNAs have several important advantages in that they are bio-developable and comprise known sequences that are often highly conserved among species, both attractive features from a drug development standpoint.

There are limitations inherent in our study. The equine model has the inability to test therapies in a large number of animals, resulting in a study that may be underpowered. This is due to the significant cost of housing, buying and caring for these animals and the strong emotional and ethical considerations in their use and sacrifice[48]. We additionally note that due to logistical and ethical considerations we were unable to completely age and sex match each animal within the treatment and placebo group. As mentioned the collagenase model of tendon injury does not totally mimic the naturally occurring lesion in man. However, the collagenase model allows the generation of a homogenous tendon lesion in a controlled group of animals and, therefore, improved ability to detect differences between treated and control arms of the study. The equine mid-metacarpal SDFT is a large, weight bearing tendon that is easily accessible, is not confined to a synovial sheath, and in the equine athlete is commonly affected by naturally occurring over-stretch tendon injury compounded on previous microfiber disruption, similar to

tendinopathies of the human Achilles tendon[49,50]. Finally, we appreciate future studies should be conducted to further elucidate the ideal time of administration of any equine tendinopathy therapy. These studies would contribute to the understanding of when the best therapeutic results are obtained and whether it is feasible to prevent further injury when the therapy is administered to a still-developing injury.

Conclusion

The present study demonstrated that a microRNA therapy had a favourable action in the treatment of tendinopathy by the prevention of the lesion progression, improved tendon tissue quality and histopathology comparable to current regenerative therapies. This data supports the mechanism of miRNA-mediated modulation of the early pathophysiologic events that facilitate tissue remodeling in tendon after injury and provides proof of principle that a locally delivered miR29a therapy can improve early tendon healing.

Contributions

N.L.M., A.E.W., D.S.G, T.H. conceived and designed the experiments. N.L.M., D.S.G, S.M.K M.A. R.R, J.G.,R.P., performed experiments T.H and I.B.M., provided expert advice. All authors analysed the data. N.L.M, A.E.W and D.S.G. wrote the paper.

Competing Interests

The authors declare no competing financial interests.

Ethical approval information

All procedures and protocols were approved by Institutional Animal Care and Use Committee, protocol number 2013-0019.

Data sharing statement

NLM, AEW, DSG have access to all the data and data are available upon request.

Methods

Equine model of tendinopathy

Animals

The data generated in Figures 1 & 2 represent historical RNA tissue samples from a previously published model[41] and were utilized in the pursuit of RRR. Eight adult female Thoroughbred (n = 7) or Thoroughbred cross (n = 1) horses, ranging in age from three to seven years, without clinical or ultrasonographic evidence of tendon injury were used. All horses had undergone rigorous athletic training prior to inclusion in the study. Horses were housed separately, in box stalls, and allowed to acclimate to the environment for ≥2 weeks prior to study initiation. These animals then underwent the tendon injury model as described below.

For the randomised section of the trial seventeen adult Quarter Horse-type horses, ranging in age from two to seven years, without clinical or ultrasonographic evidence of tendon injury were used. The sample size was based on the first authors previously published studies utilizing the collagenase model[41,51] which showed the largest group should have 8 horses to show statistically differences regarding tissue architecture, tendon size, tendon lesion size, and tendon linear fibre pattern. Horses were housed separately, in box stalls, and allowed to acclimate to the environment for ≥2 weeks prior to study initiation. All invasive procedures were performed by an experienced board certified veterinary surgeon (A.E.W). This study was approved by and performed according to guidelines of the University's Institutional Animal Care and Use Committee, protocol number 2013-0019 and all experiments were performed in accordance with relevant guidelines and regulations.

Tendon injury induction and therapy administration

Collagenase-induced lesions were created in the tensile region of the superficial digital flexor tendon (SDFT) of one randomly selected forelimb using filter sterilized bacterial collagenase type I (Sigma, St. Louis, MO, USA) as previously described[51]. Forelimb selection (left or right) was made by a coin toss for each horse. One thousand units of collagenase was delivered to a columnar physical defect centred within the tensile region of the SDFT tendon (16 to 18 cm distal to the accessory carpal bone; DACB) using a 16 gauge 8.89 cm Weiss Epidural needle with a Tuohy tip (BD, Franklin Lakes, NJ, USA) inserted under ultrasonographic guidance, as previously described. The study forelimb was bandaged. One week post tendon injury induction (0 weeks), tendons were injected with 1.5 ml of 67 µM miR29a (based on preliminary rodent in vivo studies) in PBS (modified to include 2'Fluoro and 2'O-Me nucleotides to increase half-life in serum), or placebo (PBS) via ultrasonographically-guided intra-lesional injection in the mid- metacarpal lesion with 25 gauge needle entry at 17 cm DACB, in the center of the lesion. The needle was directed from palmarolateral to dorsomedial.

Study design

The study consisted of two randomly assigned groups: group A (miRNA 29a mimic; n =9 ; 5 male, 4 female; miRNA29a) and group B (placebo treated tendons; n = 8; 4 male, 4 female; CONT). One week after tendon injury by collagenase injection, treatment injections were performed. A subset of animals were euthanized, and tissues were collected at two, four and sixteen weeks. Other than an on-site control officer, all investigators were blinded to treatment group identification until the study was completed and all assays were performed. Treatment group (A or B) was revealed for statistical analysis. Once all analyses were completed, treatment group identification (miRNA29a or CONT) was disclosed.

None of the horses had been previously athletically trained. All horses had been housed at pasture in a group setting until 2 weeks prior to the start of the study, at which point they were housed individually in box stalls until study termination. Eight weeks post treatment injection horses began daily in-hand

walking exercise for 5 minutes each day, which was increased to 10 minutes a day for weeks 12-16. There were pre-existing musculoskeletal abnormalities in 2 horses: one horse (mir29a group, 16 week horse) had a mild flexural limb deformity (club foot) and one horse had delayed release of the patella (control group, 16 week horse). One horse (mir29a group,16 week horse) got loose from her handler during the 8th week post-treatment injection and galloped free for 3 minutes. Other than one horse that was treated for colic prior to study initiation (mir29a group, week 4), none of the horses had a history of prior diseases or treatments other than castration, none required treatment for other diseases or injuries during the study and there was no evidence of prior or concomitant diseases during post mortem exam in any of the horses. The age, sex and weight of each animal is given in Table 2.

Ultrasound

Ultrasound examinations were performed prior to admission to the study (baseline) and at t = 0, 2, 4, 6, and 8, 12 and 16 weeks after treatment injection. Ultrasound imaging was performed by a board-certified internal medicine specialist (D.S.) using a hospital based non-portable ultrasound machine (MyLab 70, Esoate, Florance, Italy) equipped with a high frequency (4-13 MHz) linear array probe for equine tendon (LA523 Vet, Esoate, Florence, Italy). A template was used to ensure accurate repetition of tissue gain settings, focus, and depth of tissue penetration. Longitudinal and transverse ultrasound images were acquired and tendon cross-sectional area (TCSA), lesion cross-sectional area (LCSA), and a longitudinal linear fiber pattern score were measured by the same ultrasonographer at 16 cm DACB. The LCSA as a percentage of TCSA was calculated for relative lesion cross-sectional area (RLCSA). Tendons were also scored as having a normal shape (*yes/no*) and overlying subcutaneous thickening (*yes/no*).

Magnetic resonance imaging

Magnetic resonance imaging was performed at two, four, six, eight, twelve and sixteen weeks after treatment injection using a 3.0 Tesla MRI system

(Siemens Magnetom Verio) using a 15-channel knee coil (Quality Electrodynamics) and positioned in left lateral recumbency with a marker placed at 17 cm DACB. Sagittal and transverse plane T2 maps (i.e. turbo spin echo sequence with multiple echo times of 15.2, 30.4, 45.6, 60.8, 76, 91.2 milliseconds) and transverse plane STIR (short *tau* inversion recovery) images were acquired.

Tissue harvest

Horses were euthanized by pentobarbital overdose at two, four and sixteen weeks post treatment injection. Limbs were dissected under RNase free conditions and samples were collected from the center of the tendon lesion at 16 cm DACB extending into the surrounding normal tendon. Samples were snap-frozen in liquid nitrogen, pulverized in a freezer-mill and stored at -80℃ until use, or fixed in 4% paraformaldehyde at 4℃ f or 72 hours.

Equine tendon explants

To establish tendon explant cultures, the superficial digital flexor tendon was aseptically excised from the midmetacarpal region of both forelimbs of 3 horses (aged 2 to 5 years) without evidence or history of tendon injury; the horses were euthanized for reasons unrelated to the study. Tendons were determined to be normal on the basis of findings via palpation, gross examination, and later dissection for explant culture. Following collection, the tendon segments were maintained in culture medium during the removal of the paratenon. The tendon segments were then sectioned into 5 X 5 X 4-mm blocks and evenly distributed in 12-well plates for explant culture of tenocytes. Segments were maintained for 6 days at 37 degrees C, 5% CO_2 and 70% humidity in complete medium (penicillin [50 U/mL]; streptomycin [50 µg/mL]; ascorbic acid [100 µg/mL]; and 2% fetal bovine serum) to allow explant culture of tenocytes. After 6 days, each explant was divided, and a portion was snap-frozen in liquid nitrogen and pulverized for RNA isolation with a phenol-guanidine isothiocyanate reagent. A cross-sectional edge was fixed in 4% paraformaldehyde, embedded in paraffin, and sectioned for H&E staining. Equine tenocytes were transfected with Hsa-miR-29a-3p and miRIDIAN microRNA Negative Control #1 miRNA mimics using Dharmafect 3

(Dharmacon). Transfection efficiency was assessed using miRIDIAN™mimic Transfection control Dy-547 (Dharmacon). We determined the transfection efficiency using a fluorescently labelled miR29a mimic. This was performed initially in cultured human tenocytes where the uptake of labelled miR29a was monitored by fluorescent microscopy. Additionally, we assessed uptake of fluorescent miR29a when injected directly into the murine patellar tendon. In both cases miR29a was readily taken up by tenocytes with transfection efficiency >85%.

RNA and DNA isolation and qPCR

The cells isolated from experiments and freezer mill pulverized tendon samples from the in vivo trial were placed in Trizol before mRNA extraction. QIAgen mini columns (Qiagen) were used for the RNA clean-up with an incorporated on column DNAse step as per the manufacturer's instructions. cDNA was prepared from RNA samples according to AffinityScript (Agilent Technologies) multiple temperature cDNA synthesis kit as per the manufacturer's instructions. Real-time PCR was performed using SYBR green or Taqman FastMix (Applied Biosystems,) according to whether a probe was used with the primers. The cDNA was diluted 1 in 5 using RNase-free water. Each sample was analysed in triplicate. Primers (Integrated DNA Technologies, Belgium) were as follows:

GAPDH Fw 5'- AGAAGGAGAAAGGCCCTCAG -3' and Rev 5'- GGAAACTGTGGAGGTCAGGA -3', Beta Actin Fw 5'- AAGGGACTTCCTGTAACAATGCA -3' and Rev 5'- CTGGAACGGTGAAGGTGACA -3', Col1a1 Fw 5'- CAGACTGGCAACCTCAAGAA -3' and Rev 5'- CAGACTGGCAACCTCAAGAA -3', Col3a1 Fw 5'- CTGGAGGATGGTTGCACTAAA -3' and Rev 5'- CACCAACATCATAGGGAGCAATA -3'

All mRNA and miRNA data sets represent fold change in gene expression compared with designated control utilizing housekeeping genes GAPDH, 18S or U6 as detailed in Figure legend.

RNA isolation and quantitative PCR of miRNA

Total RNA was isolated by miRNeasy kit (Qiagen). miScript Reverse Transcription Kit (Qiagen) was used for cDNA preparation. TaqMan mRNA assays (Applied Biosystems) or miScript primer assay (Qiagen) were used for quantitative determination of the expression of miR-29a (MS00001701). Expressions of U6B small nuclear RNA or β-actin were used as endogenous controls.

Luciferase assay

Conserved miR29a binding sites in the 3'UTRs of equine col1a1 and col3a1 were identified using TargetScan. The regions corresponding to these sites were synthesised as G-blocks (Integrated DNA Technologies, Belgium) and inserted downstream of the luciferase ORF in pmiRGLO (Promega) using Gibson Assembly (New England Biolabs). The equivalent regions in which the seed regions of predicted miR29a binding sites were deleted were created in parallel. Plasmids were transfected into HEK293 cells along with miR29a or scrambled control mimics (Thermofisher) using Attractene (Qiagen). Luciferase activities were measured using Dual-Glo luciferase assay (Promega).

3' Rapid Extension of cDNA Ends

3’UTR sequences of col1a1 and col3a1 transcripts were generated by 3’ Rapid Extension of cDNA Ends (3’RACE) by using RNA prepared from equine tenocytes. The primers used were as follows: col1a1 GSP1 5'-CCCTGGAAACAGACAAACAAC -3', col1a1 GSP2 5'-CAGACAAACAACCCAAACTGAA-3', col3a1 GSP1 5'-AGGCCGTGAGACTACCTATT-3' and col3a1 5'-GSP2 CTATGATGTTGGTGGTCCTGAT-3'. The resulting PCR products were cloned into pCR2.1 TOPO (Invitrogen) for sequencing.

Histology

Fixed longitudinal tissue sections were embedded in paraffin, sectioned and stained with hematoxylin and eosin (H&E) or Picrosirius Red and examined under white light and polarized light microscopy. All slides were examined by a board certified veterinary pathologist, specialized in musculoskeletal pathology (R.P.). Sections were sequentially examined across and down the entire tendon section, under low power and high power (10 fields) where appropriate for cell detail, to derive a complete histologic impression. All tendon parameters were scored from l (normal) to 4 (severe changes) for: tenocyte shape, tenocyte density, free hemorrhage, neovascularization, perivascular cuffing, collagen fiber linearity, collagen fiber uniformity and polarized light crimping as previously described[51].

Statistical analyses

All results are shown as mean ± standard error of the mean and all statistical analysis was performed using Student's t-test, ANOVA (analysis of variance) test or Mann–Whitney test U-test, as indicated in figure legends, using the Graph Pad Prism 5 software. A p value of <0.05 was considered statistically significant.

Figure legends

Figure 1

miR29a is dysregulated in equine tendinopathy and targets col1a1 and col3a1 via conserved binding sites

(a) miR29a, (b) Col3a1 and (c) Col1a1 expression in equine tendinopathy model at 3,5,9 & 17 weeks post lesion induction. Data for mRNA are total copy number of gene versus GAPDH housekeeping gene in duplicate samples. *p<0.05, **p<0.01 versus control (ANOVA).
(d-e) sequence alignments of miR29a with its predicted binding sites in col1a1 and col3a1. Seed regions are shown in red. (f-g) Luciferase activity in HEK293 cells co-transfected with wild-type or mutated col1a1 or col3a1 3'UTR luciferase reporter and miR29a or scrambled control mimics. Activities were normalised to control and values expressed as % of scrambled controls, (n =3). Data analyzed by Mann Whitney U Test, *p<0.05 versus scrambled control

Figure 2

miR29a preferentially targets col3a1 over col1a1 in equine tenocytes

Copies col1a1 (a) and col3a1 (b) transcripts levels after transfection with miR29a and scrambled (control) mimics normalized to 10^6 copies of 18S. This was repeated in three independent experiments. **p<0.01 versus scrambled control. (Student's *t*-test). (c-d) sequence alignments of predicted col1a1 and col3a1 polyadenyation signals (underlined). (e-f) Diagram of alternative polyadenylated 3UTRs from col1a1 and col3a1, showing the positions of miR29a-binding sites and predicted polyadenylation signals (pA). (g-h) 3'RACE sequences of col1a1 and col3a1 transcripts cloned from equine tenocytes. Stop codon in red, polyA signals underlined, polyA tail in bold and miR29a binding site shown in blue.

Figure 3

miR29a treatment targets col3a1 with no effect on col1a1 in early tendon healing *in vivo*

(a) Study timeline, (b-c) Quantitative PCR of col1a1 and col3a1of tendon lesion samples expressed as copies per 10,000 copies of GAPDH. Week 2 n=3, week 4 n=2 and week 16 n=4. **p<0.01 versus scrambled control. (One way ANOVA).

Figure 4

Ultrasound tendon healing post miR29a treatment

Normalized (a) lesion and (b) lesion relative to tendon cross-sectional area (CSA) for miR29a and placebo treated tendons (control) treated tendons at time points post treatment injection in weeks. *p<0.05, versus control (one tailed Student's t-test) (c) Transverse and longitudinal ultrasound images 16 cm distal to the accessory carpal bone, sixteen weeks post treatment with miR29a or placebo treated tendons.

Figure 5

MRI tendon healing post miR29a treatment

Normalized (a) lesion to tendon cross-sectional area (CSA) for miR29a and placebo treated tendons (control) treated tendons at time points post treatment injection in weeks. (b)Transverse T_1 MR images at 17 cm distal to the accessory carpal bone sixteen weeks after treatment injection with miR29a or placebo treated tendons. (c) MRI T_2 r mapping relaxation times for miR29a and placebo treated tendons (control) at time points post treatment injection in weeks. *p<0.05, versus control (one tailed Student's t-test)

Figure 6

Histology and tissue architecture post miR29a treatment

(a) Histological scoring utilizing the modified Bonar Score (Cell density, vascularity, linear fibre and polarised collagen) at 2,4 and 16 weeks. * p<0.05 miR29a versus controls (Mann Whitney U test) (b) 200× magnification of longitudinal sections of superficial digital flexor tendon stained Picrosirius Red sixteen weeks after treatment injection with mir29a or placebo treated

tendons. Bars = 200μm. (c) Cross sectional gross pathology images from miR29a treated tendon versus control tendon at 16 weeks post treatment.

	SC Thickening		Abnormal Shape	
Weeks	29a	Control	29a	Control
0	4/9 (44)	4/8 (50)	7/9 (78)	7/8 (88)
2	4/9 (44)	4/8 (50)	8/9 (89)	7/8 (88)
4	3/7 (43)	3/6 (50)	2/7 (29)	5/6 (83)
6	3/4 (75)	4/4 (100)	2/4 (50)	4/4 (100)
8	3/4 (75)	4/4 (100)	2/4 (50)	4/4 (100)
12	1/4 (25)	3/4 (75)	2/4 (50)	4/4 (100)
16	**1/4 (25)**	**4/4 (100)**	**1/4 (25)**	**4/4 (100)**

Table 1

Subjective ultrasound scoring for subcutaneous thickening and abnormal tendon shape. Each ultrasound image was scored by a blinded assessor (D.S.) for subcutaneous thickening (*yes/no*) or abnormal tendon shape (*yes/no*) at the site of induced injury. Percentage of subjects in brackets.

Week	Group	Age	Sex	Weight(kg)	Height(cm)
2	A	4	M	413	142
2	A	3	M	394	147
2	A	3	G	412	147
2	B	4	M	468	147
2	B	6	G	558	160
4	A	6	G	404	142
4	A	6	G	432	147
4	B	2	M	492	157
4	B	2	M	484	155
16	A	3	M	408	147
16	A	2	G	424	147
16	A	2	M	436	147
16	A	4	G	466	152
16	B	4	M	452	150
16	B	3	M	402	147
16	B	6	G	420	147
16	B	2	M	443	145

Table 2

Demographics of horses utilized in study. Group A (mir29a treated), Group B (control, PBS).

References

1. Battery, L. & Maffulli, N. Inflammation in overuse tendon injuries. *Sports Med Arthrosc* **19**, 213-217 (2011).
2. Birch, H.L. Tendon matrix composition and turnover in relation to functional requirements. *Int J Exp Pathol* **88**, 241-248 (2007).
3. Dakin, S.G.*, et al.* Macrophage sub-populations and the lipoxin A4 receptor implicate active inflammation during equine tendon repair. *PLoS One* **7**, e32333 (2012).
4. Hyman, J. & Rodeo, S.A. Injury and repair of tendons and ligaments. *Scientific Principles of Sports Rehabilitaion* **11**, 267-288 (2000).
5. Goodship, A.E. The pathophysiology of flexor tendon injury in the horse. *Equine Veterinary Education* **5**, 23-29 (1993).
6. Kasashima, Y.*, et al.* Prevalence of superficial digital flexor tendonitis and suspensory desmitis in Japanese Thoroughbred flat racehorses in 1999. *Equine Vet J* **36**, 346-350 (2004).
7. Millar, N.L.*, et al.* Inflammation is present in early human tendinopathy. *Am J Sports Med* **38**, 2085-2091 (2010).
8. Millar, N.L., Dean, B.J. & Dakin, S.G. Inflammation and the continuum model: time to acknowledge the molecular era of tendinopathy. *Br J Sports Med* (2016).
9. Millar, N.L., Murrell, G.A.C. & McInnes, I.B. Inflammatory mechanisms in tendinopathy - towards translation. *Nature reviews. Rheumatology* **13**, 110-122 (2017).
10. Dakin, S.G.*, et al.* Inflammation activation and resolution in human tendon disease. *Sci Transl Med* **7**, 311ra173 (2015).
11. Behzad, H., Sharma, A., Mousavizadeh, R., Lu, A. & Scott, A. Mast cells exert pro-inflammatory effects of relevance to the pathophyisology of tendinopathy. *Arthritis Res Ther* **15**, R184 (2013).
12. John, T.*, et al.* Effect of pro-inflammatory and immunoregulatory cytokines on human tenocytes. *J Orthop Res* **28**, 1071-1077 (2010).
13. Dakin, S.G., Dudhia, J. & Smith, R.K. Science in brief: resolving tendon inflammation. A new perspective. *Equine Vet J* **45**, 398-400 (2013).
14. Dakin, S.G.*, et al.* Inflamm-aging and arachadonic acid metabolite differences with stage of tendon disease. *PLoS One* **7**, e48978 (2012).
15. Millar, N.L.*, et al.* IL-17A mediates inflammatory and tissue remodelling events in early human tendinopathy. *Sci Rep* **6**, 27149 (2016).
16. He, L. & Hannon, G.J. MicroRNAs: small RNAs with a big role in gene regulation. *Nat Rev Genet* **5**, 522-531 (2004).
17. Maurer, B.*, et al.* MicroRNA-29, a key regulator of collagen expression in systemic sclerosis. *Arthritis Rheum* **62**, 1733-1743 (2010).
18. Kurowska-Stolarska, M.*, et al.* MicroRNA-155 as a proinflammatory regulator in clinical and experimental arthritis. *Proceedings of the National Academy of Sciences of the United States of America* **108**, 11193-11198 (2011).
19. Bushati, N. & Cohen, S.M. microRNA functions. *Annu Rev Cell Dev Biol* **23**, 175-205 (2007).
20. Bartel, D.P. MicroRNAs: target recognition and regulatory functions. *Cell* **136**, 215-233 (2009).

21. Zeng, L.*, et al.* MicroRNA-210 overexpression induces angiogenesis and neurogenesis in the normal adult mouse brain. *Gene Ther* **21**, 37-43 (2014).
22. Usman, M.A.*, et al.* The effect of administration of double stranded MicroRNA-210 on acceleration of Achilles tendon healing in a rat model. *J Orthop Sci* **20**, 538-546 (2015).
23. Chen, C.H.*, et al.* Effectiveness of microRNA in Down-regulation of TGF-beta gene expression in digital flexor tendons of chickens: in vitro and in vivo study. *J Hand Surg Am* **34**, 1777-1784 e1771 (2009).
24. Chen, Q., Lu, H. & Yang, H. Chitosan inhibits fibroblasts growth in Achilles tendon via TGF-beta1/Smad3 pathway by miR-29b. *Int J Clin Exp Pathol* **7**, 8462-8470 (2014).
25. Millar, N.L.*, et al.* MicroRNA29a regulates IL-33-mediated tissue remodelling in tendon disease. *Nat Commun* **6**, 6774 (2015).
26. Brown, B.D. & Naldini, L. Exploiting and antagonizing microRNA regulation for therapeutic and experimental applications. *Nat Rev Genet* **10**, 578-585 (2009).
27. Abonnenc, M.*, et al.* Extracellular matrix secretion by cardiac fibroblasts: role of microRNA-29b and microRNA-30c. *Circ Res* **113**, 1138-1147 (2013).
28. Williams, I.F., McCullagh, K.G., Goodship, A.E. & Silver, I.A. Studies on the pathogenesis of equine tendonitis following collagenase injury. *Res Vet Sci* **36**, 326-338 (1984).
29. Lake, S.P., Ansorge, H.L. & Soslowsky, L.J. Animal models of tendinopathy. *Disabil Rehabil* **30**, 1530-1541 (2008).
30. Sengupta, S.*, et al.* MicroRNA 29c is down-regulated in nasopharyngeal carcinomas, up-regulating mRNAs encoding extracellular matrix proteins. *Proceedings of the National Academy of Sciences of the United States of America* **105**, 5874-5878 (2008).
31. Qin, W.*, et al.* TGF-beta/Smad3 signaling promotes renal fibrosis by inhibiting miR-29. *J Am Soc Nephrol* **22**, 1462-1474 (2011).
32. Ciechomska, M., O'Reilly, S., Suwara, M., Bogunia-Kubik, K. & van Laar, J.M. MiR-29a reduces TIMP-1 production by dermal fibroblasts via targeting TGF-beta activated kinase 1 binding protein 1, implications for systemic sclerosis. *PLoS One* **9**, e115596 (2014).
33. Ganal, E.*, et al.* Quantitative MRI characterization of arthroscopically verified supraspinatus pathology: comparison of tendon tears, tendinosis and asymptomatic supraspinatus tendons with T2 mapping. *Knee Surgery, Sports Traumatology, Arthroscopy* **24**, 2216-2224 (2016).
34. Bangerter, N.K., Taylor, M.D., Tarbox, G.J., Palmer, A.J. & Park, D.J. Quantitative techniques for musculoskeletal MRI at 7 Tesla. *Quantitative Imaging in Medicine and Surgery* **6**, 715-730 (2016).
35. van Schie, H.T.*, et al.* Monitoring of the repair process of surgically created lesions in equine superficial digital flexor tendons by use of computerized ultrasonography. *Am J Vet Res* **70**, 37-48 (2009).
36. Bosch, G., Moleman, M., Barneveld, A., van Weeren, P.R. & van Schie, H.T. The effect of platelet-rich plasma on the neovascularization of surgically created equine superficial digital flexor tendon lesions. *Scand J Med Sci Sports* (2010).

37. Bosch, G., Rene van Weeren, P., Barneveld, A. & van Schie, H.T. Computerised analysis of standardised ultrasonographic images to monitor the repair of surgically created core lesions in equine superficial digital flexor tendons following treatment with intratendinous platelet rich plasma or placebo. *Vet J* **187**, 92-98 (2011).
38. Garrett, K.S., Bramlage, L.R., Spike-Pierce, D.L. & Cohen, N.D. Injection of platelet- and leukocyte-rich plasma at the junction of the proximal sesamoid bone and the suspensory ligament branch for treatment of yearling Thoroughbreds with proximal sesamoid bone inflammation and associated suspensory ligament branch desmitis. *J Am Vet Med Assoc* **243**, 120-125 (2013).
39. de Vos, R.J*., et al.* Platelet-rich plasma injection for chronic Achilles tendinopathy: a randomized controlled trial. *JAMA* **303**, 144-149 (2010).
40. Nixon, A.J., Dahlgren, L.A., Haupt, J.L., Yeager, A.E. & Ward, D.L. Effect of adipose-derived nucleated cell fractions on tendon repair in horses with collagenase-induced tendinitis. *Am J Vet Res* **69**, 928-937 (2008).
41. Watts, A.E., Yeager, A.E., Kopyov, O.V. & Nixon, A.J. Fetal derived embryonic-like stem cells improve healing in a large animal flexor tendonitis model. *Stem Cell Res Ther* **2**, 4 (2011).
42. Pacini, S*., et al.* Suspension of bone marrow-derived undifferentiated mesenchymal stromal cells for repair of superficial digital flexor tendon in race horses. *Tissue Eng* **13**, 2949-2955 (2007).
43. Smith, R.K*., et al.* Beneficial effects of autologous bone marrow-derived mesenchymal stem cells in naturally occurring tendinopathy. *PLoS One* **8**, e75697 (2013).
44. Godwin, E.E., Young, N.J., Dudhia, J., Beamish, I.C. & Smith, R.K. Implantation of bone marrow-derived mesenchymal stem cells demonstrates improved outcome in horses with overstrain injury of the superficial digital flexor tendon. *Equine Vet J* **44**, 25-32 (2012).
45. Caplan, A.I. & Correa, D. The MSC: an injury drugstore. *Cell Stem Cell* **9**, 11-15 (2011).
46. Carvalho, A.M*., et al.* Equine tendonitis therapy using mesenchymal stem cells and platelet concentrates: a randomized controlled trial. *Stem Cell Research & Therapy* **4**, 85 (2013).
47. Carvalho, A*., et al.* Use of adipose tissue-derived mesenchymal stem cells for experimental tendinitis therapy in equines. *J Equine Vet Sci* **31**(2011).
48. Koch, T.G. & Betts, D.H. Stem cell therapy for joint problems using the horse as a clinically relevant animal model. *Expert Opinion on Biological Therapy* **7**, 1621-1626 (2007).
49. Abate, M*., et al.* Pathogenesis of tendinopathies: inflammation or degeneration? *Arthritis Res Ther* **11**, 235 (2009).
50. Dowling, B.A., Dart, A.J., Hodgson, D.R. & Smith, R.K.W. Superficial digital flexor tendonitis in the horse. *Equine Veterinary Journal* **32**, 369-378 (2000).
51. Watts, A.E., Nixon, A.J., Yeager, A.E. & Mohammed, H.O. A collagenase gel/physical defect model for controlled induction of superficial digital flexor tendonitis. *Equine Vet J* **44**, 576-586 (2012).

Figure 1

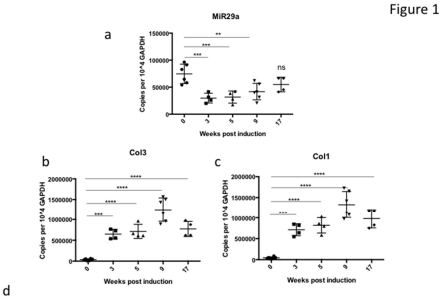

d

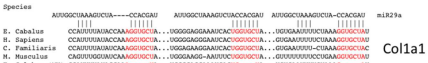

Col1a1

e

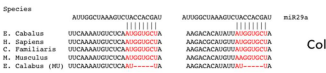

Col3a1

f

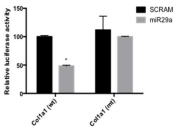

g

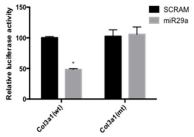

Figure 2

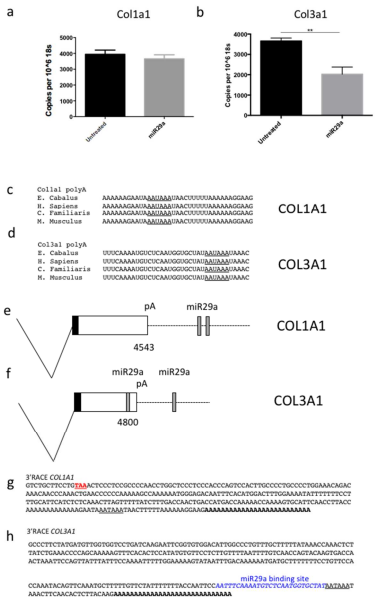
a
Col1a1
Copies per 10^6 18s
5000
4000
3000
2000
1000
0
Untreated
miR29a
b
Col3a1
**
Copies per 10^6 18s
4000
3000
2000
1000
0
Untreated
miR29a
c
Col1a1 polyA
E. Cabalus AAAAAAGAAUAAAUAAAUAACUUUUUAAAAAAGGAAG
H. Sapiens AAAAAAGAAUAAAUAAAUAACUUUUUAAAAAAGGAAG
C. Familiaris AAAAAAGAAUAAAUAAAUAACUUUUUAAAAAAGGAAG
M. Musculus AAAAAAGAAUAAAUAAAUAACUUUUUAAAAAAGGAAG
COL1A1
d
Col3a1 polyA
E. Cabalus UUUCAAAAUGUCUCAAUGGUGCUAUAAUAAAUAAAC
H. Sapiens UUUCAAAAUGUCUCAAUGGUGCUAUAAUAAAUAAAC
C. Familiaris UUUCAAAAUGUCUCAAUGGUGCUAUAAUAAAUAAAC
M. Musculus UUUCAAAAUGUCUCAAUGGUGCUAUAAUAAAUAAAC
COL3A1
e
pA
miR29a
4543
COL1A1
f
miR29a
miR29a
pA
4800
COL3A1
g
3'RACE COL1A1
GTCTGCTTCCTGTAAACTCCCCTCCGCCCCAACCTGGCTCCCTCCCACCCAGTCCACTTGCCCCTGCCCCTGGAAACAGAC
AAACAACCCAAACTGACCCCCCCAAAAAGCCAAAAAATGGGGACACAATTCACATGGACTTTGCAAAATATTTTTTTCCT
TTGCATTCATCTCTCAAACTTAGTTTTTATCTTTGACCAACTGACCATGACCAAAACCAAAAGTGCATTCAACCTTACC
AAAAAAAAAAAAAGAATAAATAAATAACTTTTTAAAAAGGAAGAAAAAAAAAAAAAAAAAAAAAAAAAAAAAA
h
3'RACE COL3A1
GCCCTTCTATGATGTTGGTGGTCCTGATCAAGAATTCGGTGTGGACATTGGCCCTGTTTGCTTTTTATAAACCAAACTCT
TATCTGAAACCCCAGCAAAAAGTTCACACTCCATATGTGTTCCTCTTGTTTTAATTTTGTCCAACCAGTACAAGTGACCA
ACTAAATTCCAGTTATTTATTTCCAAAATTTTTGGAAAAAGTATAATTTGACAAAAATGATGTCTTTTTTCCTGTTCCA
miR29a binding site
CCAAATACAGTTCAAATGCTTTTTGTTCTATTTTTTTACCAATTCCAATTTCAAAATGTCTCAATGGTGCTATAATAAAT
AAACTTCAACACTCTTACAAGAAAAAAAAAAAAAAAAAAAAAAAAAAAAAA

Figure 3

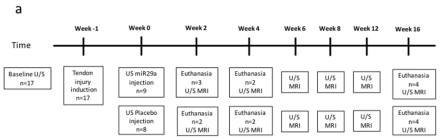
a
Time
Week -1
Week 0
Week 2
Week 4
Week 6
Week 8
Week 12
Week 16
Baseline U/S n=17
Tendon injury induction n=17
US miR29a injection n=9
US Placebo injection n=8
Euthanasia n=3 U/S MRI
Euthanasia n=2 U/S MRI
Euthanasia n=2 U/S MRI
Euthanasia n=2 U/S MRI
U/S MRI
U/S MRI
U/S MRI
U/S MRI
U/S MRI
U/S MRI
Euthanasia n=4 U/S MRI
Euthanasia n=4 U/S MRI

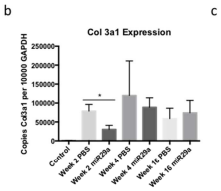
b
Col 3a1 Expression
Copies Col3a1 per 10000 GAPDH
250000
200000
150000
100000
50000
0
*
Control
Week 2 PBS
Week 2 miR29a
Week 4 PBS
Week 4 miR29a
Week 16 PBS
Week 16 miR29a

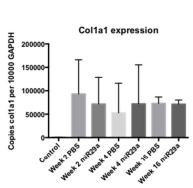
c
Col1a1 expression
Copies col1a1 per 10000 GAPDH
200000
150000
100000
50000
0
Control
Week 2 PBS
Week 2 miR29a
Week 4 PBS
Week 4 miR29a
Week 16 PBS
Week 16 miR29a

Figure 4

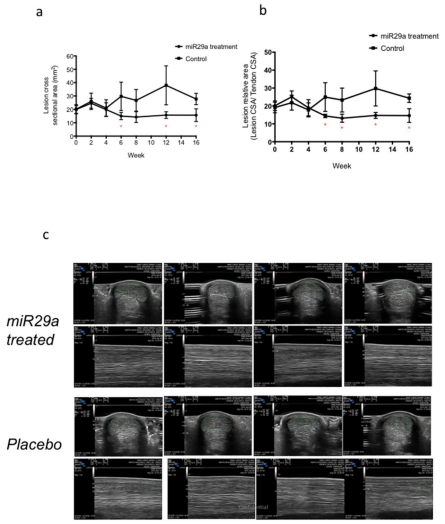
a
b
miR29a treatment
Control
Lesion cross sectional area (mm²)
Lesion relative area (Lesion CSA/ Tendon CSA)
Week
c
miR29a treated
Placebo

Figure 5

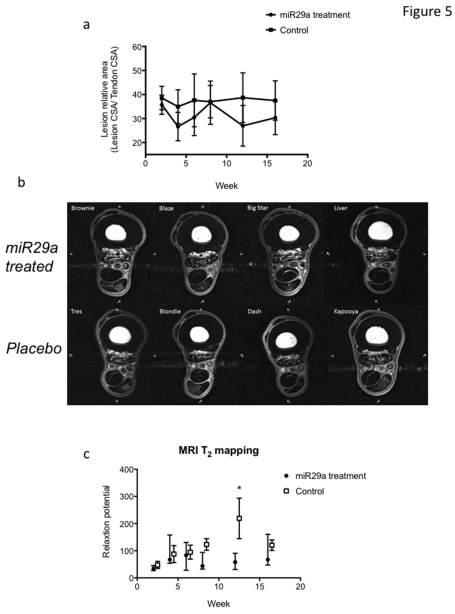
a
miR29a treatment
Control
Lesion relative area
(Lesion CSA/ Tendon CSA)
60
50
40
30
20
0
5
10
15
20
Week
b
miR29a
treated
Placebo
Brownie
Blaze
Big Star
Liver
Tres
Blondie
Dash
Kapoova
c
MRI T2 mapping
miR29a treatment
Control
Relaxtion potential
400
300
200
100
0
*
0
5
10
15
20
Week

Figure 6

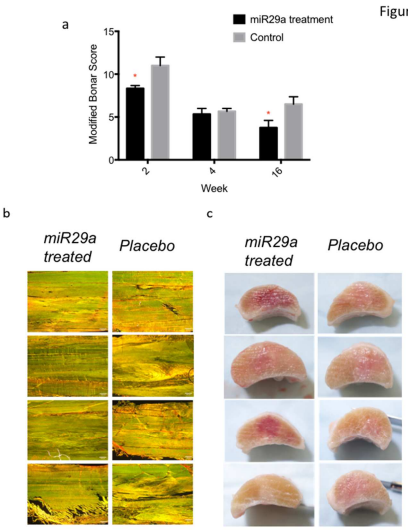
a
miR29a treatment
Control
Modified Bonar Score
15
10
5
0
2
4
16
Week
b
miR29a treated
Placebo
c
miR29a treated
Placebo